Enhancement of Phosphorescence of Ir Complexes Bound to Conjugated Polymers: Increasing the Triplet Level of the Main Chain

Gisela L. Schulz,† Xiwen Chen,† Show-An Chen,‡ and Steven Holdcroft*,†

Department of Chemistry, Simon Fraser University, Burnaby, BC, Canada V5A 1S6, and Department of Chemical Engineering, National Tsing-Hua University, Hsinchu, 30041, Taiwan, R.O.C.

Received August 9, 2006; Revised Manuscript Received October 20, 2006

ABSTRACT: Conjugated fluorene-*alt*-pyridine and fluorene-*alt*-thiophene polymers containing phosphorescent iridium complexes have been synthesized. Exchanging the 2,5-linked pyridine group with the 3,4-linked thiophene group resulted in a blue shift in the absorption and emission spectra of the conjugated polymers. Upon incorporation of the thienyl unit, phosphorescent quantum yields of films increased from 0.05 to 0.20 and electrophosphorescent external quantum efficiencies increased from 0.32 to 0.84%. These results are attributed to raising the triplet energy of the main chain polymer, with respect to the Ir phosphor, thereby reducing quenching of the phosphor by the main chain.

Introduction

Recently, much effort has been invested into developing organic light-emitting devices (OLEDs). Conjugated polymers are attractive for such applications because of their solution processability, mechanical flexibility, color tunability, and low operating voltage.[1,2] Commonly, light emission from conjugated polymers is fluorescent; however, systems that emit phosphorescence have gained interest because of the potential for higher EL efficiencies, resulting from emission of both singlet and triplet excitons. Heavy metal complexes promote spin−orbit coupling of electronic states, resulting in rapid intersystem crossing (ISC), short triplet state lifetimes, and stronger phosphorescent emission at room temperature.

Phosphorescent OLEDs based on "small" molecules have received the most attention to date. Organometallic complexes of Pt, Ir, Ru, Re, and Os have all been investigated to various extents as the emitting species in phosphorescent OLEDs.[3−7] It has been shown that the emission wavelength can be tuned by changing the ligands attached to the metal center. Nevertheless, the use of small organic molecules requires vacuum deposition of multilayer structures, a process that increases fabrication costs. In an attempt to mitigate the need for vacuum deposition processes, small molecules have been doped into polymer matrices. These systems are solution processable and, in principle, allow for easy deposition of multiple layers. Examples of such systems include poly(vinylcarbazole) (PVK) doped with $Ir(ppy)_3$,[8] blends of PVK and 2-*tert*-butylphenyl-5-biphenyl-1,3,4-oxadiazol (PBD) doped with tris(2,5-bis-2′-(9,9-dihexylfluorene)pyridine)iridium(III) ($Ir(HFP)_3$),[9] and poly(9,9-dioctylfluorene) (PFO) doped with $Ir(ppy)_3$.[10]

Although significant improvements in device efficiencies using blended systems are reported, their performance can suffer from aggregation of the phosphor, phosphorescent quenching,[11] phase separation, and inefficient energy transfer.[12] In efforts to overcome these shortcomings, a new class of materials, in which phosphorescent groups are covalently attached to a conjugated polymer backbone, are being investigated. Chen et al.[13] reported the first synthesis of such materials and showed that polyfluorene with pendent iridium complexes ($Ir(ppy)_2acac$ and $Ir(btp)_2(acac)$) and charge transport moieties (carbazole) have comparable efficiencies to Ir complex-based OLEDs. Jiang et al.[14] developed a similar system of fluorene-*alt*-carbazole polymers with various ligands bound to iridium pendent groups attached to the N-position of the carbazole, for example, 1-phenylisoquinoline, 2-naphthylpyridine, and 2-phenylquinoline. They attribute the observed increase in device performance to the high triplet energy of carbazole and efficient charge injection due to a more favorable position of the HOMO and LUMO levels. Sandee et al. developed a synthetic strategy to covalently attach phosphorescent emitters [$Ir(ppy)_2(acac)$ and $Ir(btp)_2(acac)$] to a poly(9,9-dioctylfluorene) backbone.[11] The latter confirmed work by Sudhakar (using a fluorene trimer) that revealed the importance of the relative triplet energy levels of the donor and acceptor on the intensity of phosphorescent emission.[15] A similar study by Zhen et al.[12] describes the synthesis and characterization of poly(fluorene-*co*-carbazole) containing varying mole fractions of iridium phosphors attached to the polymer backbone. This study emphasized the improvement of iridium bound polymers compared to their corresponding blend systems, attributing it to the more efficient intramolecular energy transfer of the former vs intermolecular energy transfer of the latter. Work by Yang et al.[16] described hyperbranched and linear substituted poly(*p*-phenylene)s based on $Ir(ppy)_3$ and $(mppy)_2Ir(acac)$ complexes. In addition, a conjugated fluorene-based polymer with an iridium complex covalently attached to the polymer main chain was described by Ito et al.[17] The iridium content in this system was optimized by its blending with 4,4′-*N*,*N*′-carbazole-biphenyl (CBP) and 2-*tert*-butylphenyl-5-biphenyl-1,3,4-oxadiazole (PBD). The systems described above all indicate that phosphorescent groups bound to conjugated polymers are promising candidates for PLEDs and provided the impetus for this current study on reduction of phosphorescent quenching. Understanding quenching pathways of phosphorescent species by main chain, conjugated polymer triplet states is necessary in order to refine the design of highly efficient systems. Several studies have examined the role of the triplet energy of the phosphor on the efficiency of quenching but none have examined the role of modifying the energy levels of the main chain. In this report, we examine the effect of modifying the triplet energy of the polymer main chain with a view to reducing triplet quenching

† Simon Fraser University.
‡ National Tsing-Hua University.
* Corresponding author: E-mail: holdcrof@sfu.ca.

10.1021/ma061814o CCC: $33.50
Published on Web 12/05/2006

Scheme 1. Depiction of Energy Transfer between a Conjugated Polymer Backbone and a Phosphor and Subsequent Quenching of the Triplet State by the Polymer Backbone.

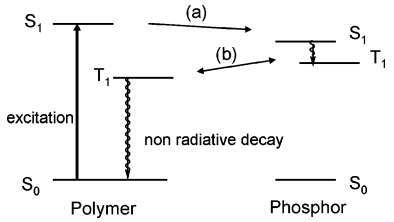

Scheme 2. Generalized Structures of the Polymers Used in This Study

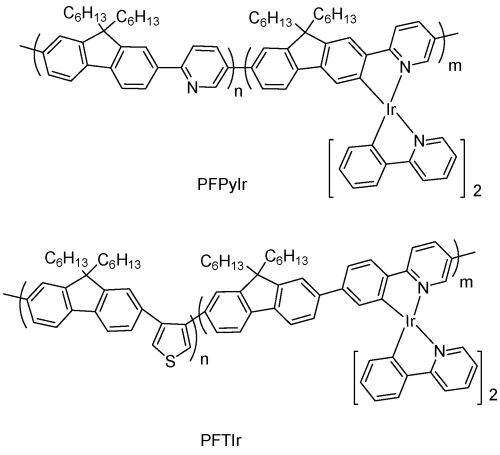

of phosphorescent complexes by the main chain. This is achieved through the design, synthesis, and characterization of polymer structures of the type below **(**Scheme 2**)**, wherein an iridium complex, of varying mole fractions, is attached to the main chain of a conjugated polymer. The conjugated polymer is designed with and without 3,4-linked thienyl groups which, when incorporated, are expected to lower conjugation along the backbone,[19] thereby increasing the electronic energy levels (both singlet and triplet) of the main chain. By changing the mole fraction of the iridium complex along the chain, it is also found that the energy levels of the phosphor can be favorably tuned to reduce triplet quenching, i.e., lowered, without affecting the energy levels of the main chain.

Experimental Section

Materials and Chemicals. 9,9-Dihexylfluorene-2,7-bis(trimethyleneborate), 2,5-dibromopyridine, 3,4-dibromothiophene, tetrakis-(triphenylphosphine)palladium ($Pd(PPh_3)_4$), 2,5-dibromobenzene, iridium(III) chloride trihydrate, and cresyl violet perchlorate were purchased from either Aldrich or Acros. THF and ether were dried over sodium and freshly distilled before use. Poly(styrenesulfonic acid)-doped poly(ethylenedioxythiophene) (PEDOT:PSS, Baytron P CH 8000) was purchased from Bayer.

Synthesis of PFPyIr. 9,9-Dihexylfluorene-2,7-bis(trimethyleneborate) was copolymerized with 2,5-dibromopyridine by Suzuki coupling to produce an alternating copolymer, PFPy. The polymers were subject to two postfunctionalization reactions in order to attach the iridium complex and produce PFPyIr (Scheme 3).

Synthesis of PFTIr. Iridium(III) chloride trihydrate was reacted with 2-phenylpyridine to produce a chloride-bridged dimer. The product was then reacted with 2 equiv of 1,4′-dibromo-2-phenylpyridine to yield $(ppy)_2Ir(BrPhPyBr)$. 9,9-Dihexylfluorene-2,7-bis-(trimethyleneborate) was copolymerized with a varying ratio of 3,4-dibromothiophene and $(ppy)_2Ir(BrPhPyBr)$ using Suzuki coupling to produce the alternating copolymer, PFTIr(ppy) (Scheme 4).

Poly(9,9-dihexylfluorene-*alt*-pyridine) (PFPy) was synthesized via Suzuki polycondensation according to Scheme 3.[18] 9,9-Dihexylfluorene-2,7-bis(trimethyleneborate) (1.0 g, 2.0 mmol) and 2,5-dibromopyridine (0.47 g, 2.0 mmol) were dissolved in THF (12.5 mL, deoxygenated), to which a solution of K_2CO_3 (0.19 g/mL, 2 mL) was added, together with $Pd(PPh_3)_4$ (0.076 g, 3 mol % based on fluorene). The resulting mixture was sealed in a glass vial and heated for 24−72 h at 80 °C in an oil bath. End-capping of the polymer was carried out as the last step in synthesis. Phenylboronic acid (0.012 g, 5 mol %) was added, and the solution was heated (80 °C, 8 h). This was followed by the addition of bromobenzene (0.016 g, 5 mol %), and the temperature was maintained at 80 °C (16 h). Once cooled to room temperature, the THF was removed and the residue was dissolved in chloroform. This was followed by washing with water (3 times) and drying over anhydrous magnesium sulfate. After filtration, the volume of chloroform was reduced, and the concentrated solution was passed through an alumina column. The volume of the resulting solution was again reduced and precipitated in methanol (∼50 mL) to yield 0.58 g of the product (78%). A weight-average molecular weight (M_w) of 44 000 Da and a PDI of 1.6 were obtained. ^{1}H NMR (CD_2Cl_2) δ (ppm): 9.09 (s, 1H), 8.20−7.75 (m, 8H), 2.13 (br β-CH_2), 1.15−0.78 (m, CH_2 and CH_3). Anal. Calcd for $(C_{25}H_{32})_{0.5}(C_5H_3)_{0.5}$: C, 87.97; H, 8.61; N, 3.42. Found: C, 87.56; H, 8.61; N, 3.52.

General Procedure for the Synthesis of PFPyIr5, PFPyIr10, PFPyIr15, PFPyIr20, and PFPyIr30 Using PFPyIr5 as an Example.[20] Poly(9,9-dihexylfluorene-*alt*-pyridine) (43.5 mg, 0.106 mmol) was reacted with $Ir(acac)_3$ (2.6 mg, 0.0053 mmol) in *m*-cresol (10 mL, degassed) at 250 °C for 10 h. After cooling, 2-phenylpyridine (1.6 mg, 0.011 mmol) was added to the solution and reacted for an additional 10 h at 250 °C.[21] The volume of the obtained solution was reduced to ∼1 mL and precipitated from methanol three times. Purification was carried out using flash chromatography using silica gel and a mixture of dichloromethane and pyridine as the eluent. ^{1}H NMR (CD_2Cl_2) δ (ppm): 9.09 (s), 8.20−7.75 (m), 2.13 (br β-CH_2), 1.15−0.78 (m, CH_2 and CH_3). A weight-average molecular weight (M_w) of 28 500 Da and a PDI of 2.1 were obtained.

PFPyIr10. ^{1}H NMR (CD_2Cl_2) δ (ppm): 9.09 (s), 8.20−7.75 (m), 2.13 (br β-CH_2), 1.15−0.78 (m, CH_2 and CH_3). A weight-average molecular weight (M_w) of 44 000 Da and a PDI of 1.7 were obtained.

PFPyIr15. ^{1}H NMR (CD_2Cl_2) δ (ppm): 9.09 (s), 8.20−7.75 (m), 2.13 (br β-CH_2), 1.15−0.78 (m, CH_2 and CH_3). A weight-average molecular weight (M_w) of 47 000 Da and a PDI of 1.9 were obtained.

PFPyIr20. ^{1}H NMR (CD_2Cl_2) δ (ppm): 9.09 (s), 8.20−7.75 (m), 2.13 (br β-CH_2), 1.15−0.78 (m, CH_2 and CH_3). A weight-average molecular weight (M_w) of 35 000 Da and a PDI of 1.9 were obtained.

PFPyIr30. ^{1}H NMR (CD_2Cl_2) δ (ppm): 9.09 (s), 8.20−7.75 (m), 2.13 (br β-CH_2), 1.15−0.78 (m, CH_2 and CH_3). A weight-average molecular weight (M_w) of 25 300 Da and a PDI of 2.6 were obtained.

$[(ppy)_2IrCl]_2$. $[(ppy)_2IrCl]_2$ was synthesized according to a modified published procedure.[23] Iridium(III) chloride trihydrate (0.150 g, 0.502 mmol) and 2-phenylpyridine (0.779 g, 5.02 mmol) were dissolved in ethylene glycol (10 mL). The reaction flask was subjected to microwave energy (2450 MHz, 480 W) under nitrogen for 35 min. After cooling, the solvent volume was reduced under vacuum to yield a yellow precipitate, which was collected on a glass filter frit. The precipitate was washed with 95% ethanol (20 mL) and acetone (20 mL) and dissolved in dichloromethane (30 mL). Toluene (12 mL) and hexanes (5 mL) were added to the dichloromethane, which was then reduced in volume and cooled to yield dark yellow crystals (0.160 g, 60%). ^{1}H NMR (CD_2Cl_2) δ (ppm): 9.23 (d, 1H), 7.78 (d, 1H), 7.67 (t, 1H), 7.39 (d, 1H), 6.67 (m, 2H), 6.50 (t, 1H), 5.90 (d, 1H). MS (MALDI): *m*/*z* 1070.87 (M/z), 1034.99 (M/z − Cl), 501.19 (M/z − $Cl_2Ir(ppy)_2$).

1,4′-Dibromo-2-phenylpyridine was synthesized according to published procedures.[22] To a suspension of magnesium turnings (0.230 g, 9.4 mmol) in 5 mL of ether, 2,5-dibromobenzene (2.170 g, 9.2 mmol) in 10 mL of ether was added dropwise at room

Scheme 3. Synthetic Route for PFPyIr

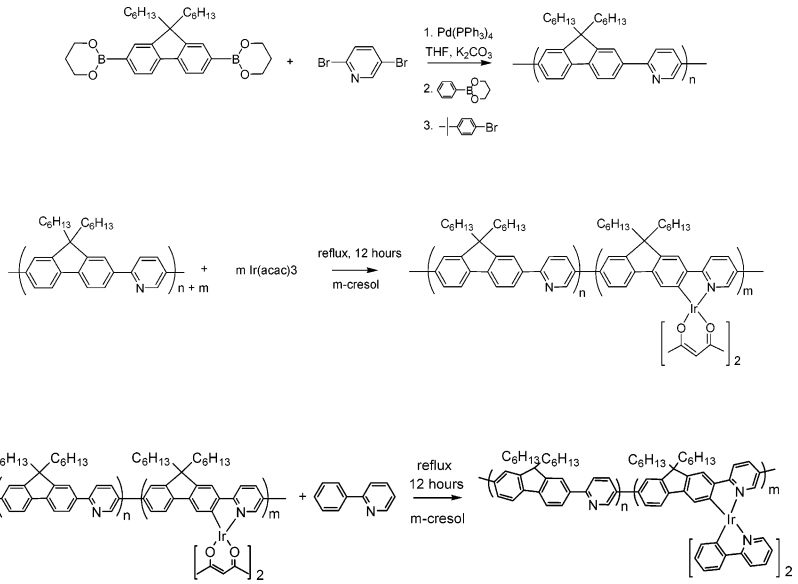

Feed ratio	PFPy	PFPyIr5	PFPyIr10	PFPyIr15	PFPyIr20	PFPyIr30
n/ m	1/ 0	0.95/ 0.05	0.90/ 0.10	0.85/ 0.15	0.80/ 0.20	0.70/ 0.30

Scheme 4. Synthetic Route for PFTIr

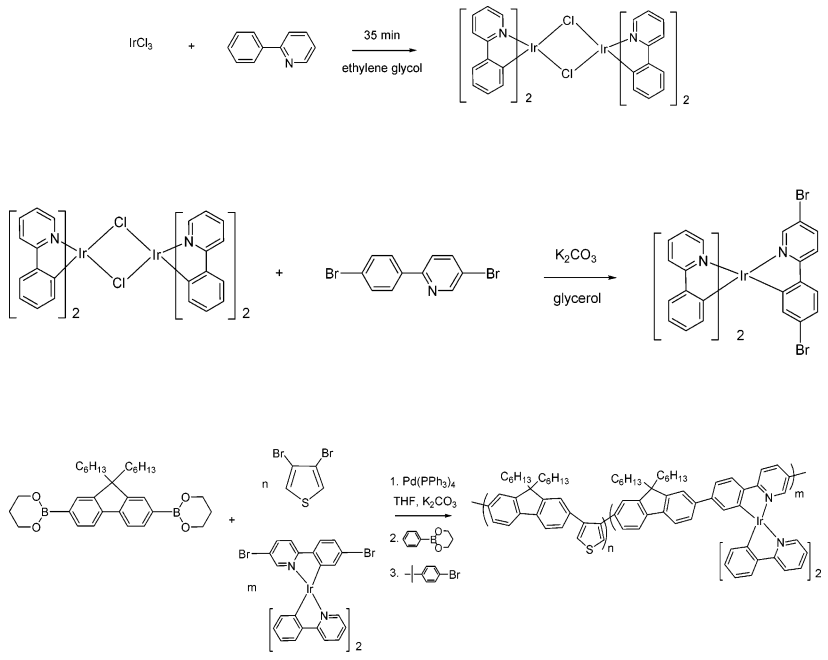

Feed ratio	PFT	PFTIr2	PFTIr5	PFTIr10	PFTIr20
n/ m	1/ 0	0.98/ 0.02	0.95/ 0.05	0.90/ 0.10	0.80/ 0.20

temperature. The resulting mixture was stirred at room temperature until all the magnesium was consumed (∼4 h). The mixture was then added to a mixture of 2,5-dibromopyridine (2.298 g, 9.7 mmol) and $PdCl_2$ (dppb) (0.061 g, 0.10 mmol) at room temperature and stirred overnight. The solvent was removed, and water was added to the residue (100 mL), followed by dilute HCl until the pH of the solution reached 5. The product was extracted with chloroform (3 × 30 mL), washed with water, and dried over anhydrous magnesium sulfate. Column chromatography was used to isolate the product (silica gel, hexane, and a mixture of hexane and ether, 15:1), which was recrystallized from a mixture of chloroform and hexane. Fluffy, white crystals were obtained (0.9755 g, 33%). ^{1}H

Table 1. Summary of Photophysical Data for PFPyIr

	solution		film		
polymer	absorption λ_{max} (nm)	emission λ_{max} (nm)	absorption λ_{max} (nm)	emission λ_{max} (nm)	Φ_{film}[a]
PF[23,28]	379	415	385.5	422	0.12
PFPy	391	416 (442)	394	428 (453)	
PFPyIr5	391	416 (442, 610)	396	613 (423,453, 665)	0.040
PFPyIr10	391	416 (442, 610)	396	613 (423,665, 453)	0.050
PFPyIr15	391	416 (442, 610)	396	613 (423,665, 453)	0.037
PFPyIr20	391	416 (442, 610)	396	613 (423,665, 453)	0.045
PFPyIr30	391	416 (442, 610)	396	613 (423,665, 453)	0.045
$Ir(ppy)_3$[3]	385 (450)	515	390 (455)	518	0.12

[a] Triplet emission, except PF and PFPy.

Table 2. Summary of Photophysical Data for PFTIr Series

	solution		film		
polymer	absorption λ_{max} (nm)	emission λ_{max} (nm)	absorption λ_{max} (nm)	emission λ_{max} (nm)	Φ_{film}[a]
PFT	323	380	326 (304)	390 (410)	0.07
PFTIr2	323 (300)	382	328 (306)	553 (390,410)	0.14
PFTIr5	325 (300)	386	327 (306)	554 (410)	0.21
PFTIr10	323 (300)	386	327 (306)	570	0.22
PFTIr20	324 (300)	387	329 (303)	573	0.23
Ir(ppy)37	385 (450)	515	390 (455)	518	0.12

[a] Triplet emission, except PFT.

NMR ($CDCl_3$) δ (ppm): 8.73 (d, 1H), 7.88 (dd, 1H), 7.85 (s, 1H), 7.83 (s, 1H), 7.59−7.61 (s, 3H). MS (EI): *m*/*z* 315, 313, 311 (M^+, 1:2:1).

$(ppy)_2Ir(BrPhPyBr)$ was synthesized according the published procedures.[24] $[(ppy)_2IrCl]_2$ (0.150 g, 0.14 mmol) and 1,4′-dibromo-2-phenylpyridine (0.109 g, 0.35 mmol) were dissolved in glycerol (10 mL) with K_2CO_3 (0.193 g). The reaction was carried out under an inert atmosphere at 200 °C for 22 h. After cooling, deionized water (20 mL) was added to the reaction mixture, which resulted in precipitation of the product, which was subsequently washed with ether and hexanes. Further purification was performed using flash chromatography (silica gel, CH_2Cl_2). Addition of methanol to the chromatographed solution followed by removal of the dichloromethane resulted in precipitation of an orange powder (0.090 g, 40% yield). ^{1}H NMR (CD_2Cl_2) δ (ppm): 7.84 (d, 1H), 7.59 (m, 2H), 7.48 (m, 1H), 6.84 (m, 2H), 6.67 (m, 2H). MS (MALDI): *m*/*z* 807.26 (M/z), 655.23 (M/z − ppy).

Poly(9,9-dihexylfluorene-*alt*-3,4-thiophene) (PFT) was synthesized via Suzuki polycondensation according to Scheme 4.[18,19] 9,9-Dihexylfluorene-2,7-bis(trimethyleneborate) (0.53 g, 1.00 mmol) and 3,4-dibromothiophene (0.26 g, 1.00 mmol) were dissolved in THF (10 mL, degassed), to which a solution of K_2CO_3 (0.19 g/mL, 2 mL) was added, together with $Pd(PPh_3)_4$ (0.036 g, 3 mol % based on fluorene). The resulting mixture was sealed in a glass vial and heated for 24−72 h at 80 °C in an oil bath. The solution obtained was washed with water (three times) and dried over anhydrous magnesium sulfate. After filtration, the volume of chloroform was reduced and passed through an alumina column. The volume of the resulting solution was reduced and precipitated in methanol (∼25 mL) to give 0.332 g (yield, 80%). A weight-average molecular weight (M_w) of 8132 Da and a PDI of 1.3 were obtained. ^{1}H NMR (CD_2Cl_2) δ (ppm): 7.7−7.1 (8H, fluorene and thiophene), 1.7 (4H, β-CH_2), 1.05 (12H, CH_2), 0.70 (6H, CH_3), 0.55 (4H, CH_2). Peaks were assigned using the ^{1}H NMR spectra of 9,9-dihexylfluorene-2,7-bis(trimethyleneborate) and 3,4-dibromothiophene. Anal. Calcd for $(C_{25}H_{32})_{0.5}(C_4H_2S)_{0.5}$: C, 84.0; H, 8.26. Found: C, 84.23; H, 8.20.

General Procedure for the Synthesis of PFTIr2, PFTIr5, PFTIr10, and PFTIr20 Using PFTIr5 as an Example. Suzuki polycondensation: 9,9-Dihexylfluorene-2,7-bis(trimethyleneborate) (0.307 g, 0.61 mmol), 3,4-dibromothiophene (0.140 g, 0.58 mmol), and $(ppy)_2Ir(BrPhPyBr)$ (0.024 g, 0.03 mmol) were dissolved in THF (10 mL, degassed), to which a solution of K_2CO_3 (0.19 g/mL, 2 mL) was added, together with $Pd(PPh_3)_4$ (0.022 g, 3 mol % based on fluorene). The resulting mixture was sealed in a glass vial and heated for 24−72 h at 80 °C in an oil bath. End-capping of the polymer was carried out as the last step in synthesis. Phenylboronic acid (0.004 g, 5 mol %) was added, and the solution was heated (80 °C, 8 h). This was followed by the addition of bromobenzene (0.016 g, 5 mol %) which was heated at 80 °C for 16 h. The solution was washed with water (three times) and dried over anhydrous magnesium sulfate. After filtration, the volume of chloroform was reduced and passed through an alumina column. The volume of the resulting solution was again reduced and precipitated in methanol (∼50 mL) to yield 0.100 g of product (yield, 37%). ^{1}H NMR (CD_2Cl_2) δ (ppm): 7.93−6.75 (m, 9H), 1.69 (br 4H), 1.15−0.52 (m, 22H). Peaks were assigned using the ^{1}H NMR spectra of 9,9-dihexylfluorene-2,7-bis(trimethyleneborate), 3,4-dibromothiophene, and $Ir(ppy)_3$. A weight-average molecular weight (M_w) of 3300 Da and a PDI of 1.9 were obtained.

PFTIr2. Yield of 0.100 g (32%). ^{1}H NMR (CD_2Cl_2) δ (ppm): 7.93−6.75 (m, 9H), 1.69 (br 4H), 1.15−0.52 (m, 22H). A weight-average molecular weight (M_w) of 5700 Da and a PDI of 2.1 were obtained.

PFTIr10. Yield of 0.175 g (53%). ^{1}H NMR (CD_2Cl_2) δ (ppm): 7.93−6.75 (m, 9H), 1.69 (br 4H), 1.15−0.52 (m, 22H). A weight-average molecular weight (M_w) of 7010 Da and a PDI of 1.9 were obtained.

PFTIr20. Yield of 0.217 g (69%). ^{1}H NMR (CD_2Cl_2) δ (ppm): 7.93−6.75 (m, 9H), 1.69 (br 4H), 1.15−0.52 (m, 22H). A weight-average molecular weight (M_w) of 6550 Da and a PDI of 2.0 were obtained.

Characterization. Solutions of the polymers used for acquiring absorption and fluorescence spectra were prepared from freshly distilled THF. Chloroform (spectro-grade, Caledon Laboratories Ltd.) was used to prepare solutions (4 mg/mL) for film casting. Films were spin-cast on either quartz or glass slides at 1500 rpm for 60 s. NMR spectroscopy was performed using a 400 MHz Bruker AMX400 spectrometer. Elemental analyses were performed using a Carlo Erba model 1106 CHN analyzer. Molecular weight determinations were performed using gel permeation chromatography (Waters model 1515 isocratic pump). Polymers were eluted with THF using a flow rate of 1 mL/min and monitored with a UV−vis detector (Waters 2487). Microwave synthesis was performed using an in-house modified Panasonic Inverter microwave (model no. NN-S614). Absorption and fluorescence spectra were collected using Cary 3E and PTI spectrophotometers, respectively. Quantum yield measurements were performed using an integrating sphere. Electroluminescence spectra were collected using a Jobin Yvon Horiba, Fluoromax-3 fluorescence spectrometer. Mass spectrometry was performed using a Voyager DE Perceptive biosystems MALDI spectrometer. Cyclic voltammograms were measured on

polymer films drop cast on a Pt disk electrode (1.5 mm) in acetonitrile containing 0.1 M Bu_4NClO_4, a Pt wire counter electrode, and a scan rate of 50 mV/s. Potentials were measured against an Ag/AgCl reference electrode and reported against ferrocene/ferrocenium using a potentiostat/galvanostat (PAR 263A). Quantum yields of the iridium containing polymers were measured against a standard using the following equation[25]

$$\Phi_u = [(\Phi_s/\Phi_{cs})]\Phi_{cu} \quad (1)$$

where Φ_u is the quantum yield of the unknown, Φ_s is the quantum yield of the standard , Φ_{cs} is the quantum yield of the standard calculated using the integrating sphere, and Φ_{cu} is the quantum yield of the unknown calculated using the integrating sphere. Cresyl violet perchlorate was selected as the standard. Its quantum yield is reported to be 0.54 ± 0.03 in methanol.[9]

The following electroluminescent device configurations were used: ITO/PEDOT:PSS/conjugated polymer/CsF (2.0 nm)/Al (60 nm) and ITO/PEDOT:PSS/conjugated polymer/TPBI (30 nm)/CsF (2.0 nm)/Al (60 nm). ITO patterned glass was precleaned, followed by O_2 plasma treatment (45 W, 193 mbar, 5 min). PEDOT:PSS (Bayer) was spin-coated at 2000 rpm for 90 s, and the layer was dried under vacuum for 1 h at 140 °C. Solutions of the conjugated polymers were spin-coated on the PEDOT:PSS layer from $CHCl_3$ solutions (~8 mg/mL) to yield films 800−1100 Å thick. CsF and Al layers were thermally evaporated at a pressure $<10^{-6}$ Torr, yielding thicknesses of 2.0 and 60 nm, respectively. The electrical and luminescence properties of devices were measured using a Keithley power supply (model 238) and a luminescence meter (BM8 from TOPCON), respectively. Polymer thicknesses were determined using a Tencor P-10 surface profiler. The active area of the diode was ~10 mm^2.

Results and Discussion

1. Synthesis and Properties of PFPyIr. Scheme 3 depicts the Suzuki polycondensation reaction that yielded poly(9,9-dihexylfluorene-*alt*-pyridine). Two subsequent postfunctionalization reactions attached the iridium complex with the desired ligands. The feed ratios of iridium complexes in the postfunctionalization reaction were 0, 5, 10, 15, 20, and 30 mol %; the corresponding polymers are termed PFPy, PFPyIr5, PFPyIr10, PFPyIr15, PFPyIr20, and PFPyIr30, respectively. The weight-average molecular weights were determined to be between 25 000 and 47 000 with polydispersity ranging from 1.6 to 2.6.

Absorption and Photoluminescent Properties. Absorption and emission wavelengths of poly(9,9-dihexylfluorene) (PF) and poly(9,9-dihexylfluorene-*alt*-2,5-pyridine) (PFPy), listed in Table 1, are similar (385 vs 394 nm and 422 vs 428 nm for solid state absorption and photoluminescence, respectively), indicating that the pyridine groups do not significantly perturb the energy gap of polyfluorene. The solid state absorption and photoluminescence spectra are slightly red-shifted relative to those obtained in solution due to aggregation.[26] Peak assignments were made by comparing the absorption spectra of poly(fluorene), PFPy, PFPyIr, and $Ir(ppy)_3$ (Figure 1). The absorption maximum of PF, PFPy, and the iridium containing polymers (PFPyIr) (Figure 1 and Table 1) are similar, but that of $Ir(ppy)_3$ differs. $Ir(ppy)_3$ has a strong absorption in the UV region attributed to the $\pi-\pi^*$ transition.[3,21] In addition, weaker ^{1}MLCT and ^{3}MLCT bands are observed for $Ir(ppy)_3$ at 390 and 455 nm, respectively.[3,27] Since PFPy and PFPyIr exhibit a single absorption peak at 391 and 396 nm in the solution and solid state, respectively, it is concluded that the polymer backbone is responsible for absorption in these systems. Figure 2 shows emission spectra of PFPyIr polymers illustrating that the luminescence intensity associated with fluorescence from the backbone decreases with increasing iridium content. For polymers bearing iridium complexes, an emission peak is observed at 610 nm in solution and 613 nm in the solid state. This peak is due to phosphorescence from the iridium complex[11] which is a result of energy transfer from the excited singlet state of the polymer backbone to the excited singlet state of the Ir complex, followed by intersystem crossing to the triplet state of the Ir complex and subsequent emission (phosphorescence) from this state,[9] as depicted in Scheme 1. Quantum yields of phosphorescence are too low for accurate measurement in solution, but they increase considerably in the solid state. However, the quantum yield of phosphorescence from these films is relatively low (~0.05), regardless of the iridium content in the polymer (see Table 1).

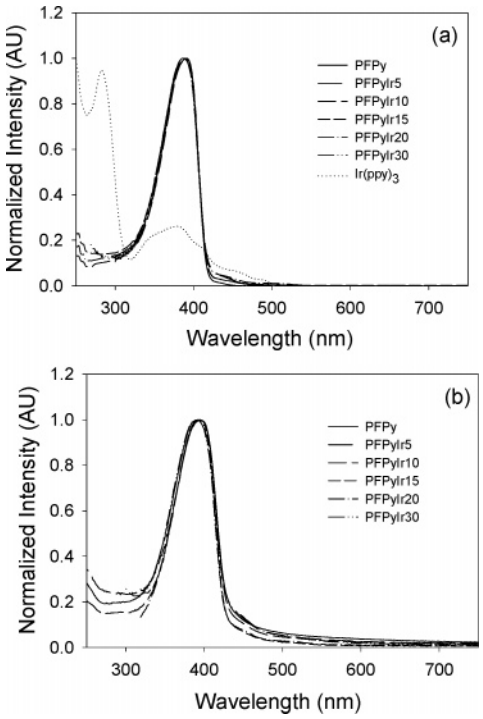

Figure 1. Absorption spectra of PFPyIr in solution (a) and as a film (b).

Triplet Energy Levels. The HOMO energy level of PFPy, depicted in Scheme 5, was estimated using cyclic voltammetry and was found to be in agreement with previously reported values.[28] The LUMO energy level was calculated from the HOMO energy level and the onset of the absorption. The triplet energy gap of the polymer was estimated using the following equation: $T_1 = (1.13S_1 - 1.43) \pm 0.25$ eV.[31] The ground state energy level of the iridium complex attached to PFPy is approximated to be between 5.2 eV ($Ir(ppy)_3$)[30] and 4.73 eV ($Ir(HFP)_3$ (tris(2,5-bis-2′-(9,9-dihexylfluorene)pyridine)iridium-(III))[9] due to the similarity of their chemical structures. The structure of one of the ligands bound to the iridium center is similar to that in HFP, and the other two ligands are identical to ppy. The triplet energy of the phosphor was estimated from the phosphorescent emission wavelength (609 nm, 2.04 eV). Scheme 5 indicates the triplet energy of PFPy to be 2.13 eV. It is believed that this low-energy gap results in quenching of the excited triplet state of the iridium complex by energy transfer to the triplet of the polymer backbone. This would result in quenching of emission from the phosphor and explains the corresponding low quantum efficiencies (0.05) for the PFPyIr series. Previous work[15] indicates that the emission quenching of the phosphor may be reduced by decreasing the triplet energy of the phosphor (guest) relative to the polymer (host). We have taken a different approach and modified the PFPy series with

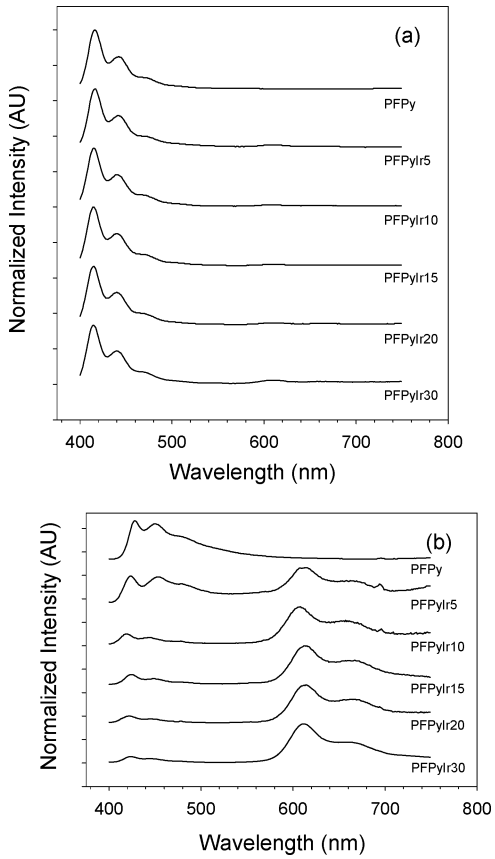

Figure 2. Photoluminescence spectra of PFPyIr in solution (a) and as a film (b).

Scheme 5. Energy Level Diagram (eV) of PFPyIr and PFTIr

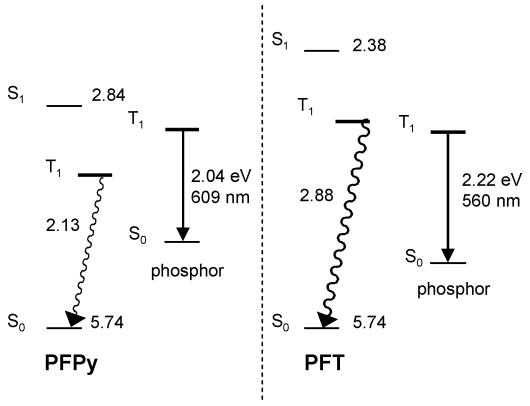

aim of increase the triplet energy of the host polymer so that triplet energy transfer from the phosphor to the triplet backbone is less favorable. A new series of Ir-containing polymers containing a 3,4-linked thienyl moiety, PFTIr, were designed to test this hypothesis. As will be demonstrated in the following sections, the triplet energy of the conjugated polymer backbone was raised by 0.75 eV, as illustrated in Scheme 5.

2. Synthesis and Properties of PFTIr. Scheme 4 depicts the synthetic route used to prepare iridium-containing monomers via the corresponding iridium chloride-bridged dimers. Monomer synthesis was carried out using an in-house modified microwave oven. The Suzuki polycondensation method was used to prepare polymers with the following iridium contents: 0, 2, 5, 10, and 20 mol %. The corresponding polymers were named PFT, PFTIr2, PFTIr5, PFTIr10, and PFTIr20, respectively. The weight-average molecular weights were determined to be between 3300 and 8100 with polydispersity ranging from 1.3 to 2.1. The low molecular weights of the PFTs are believed to be due to the low reactivity of the 3,4-dibromothiophene relative to the 2,5-dibromopyridine. Previous reports of poly(fluorene-*co*-thiophene)s had similar molecular weights.[19,33]

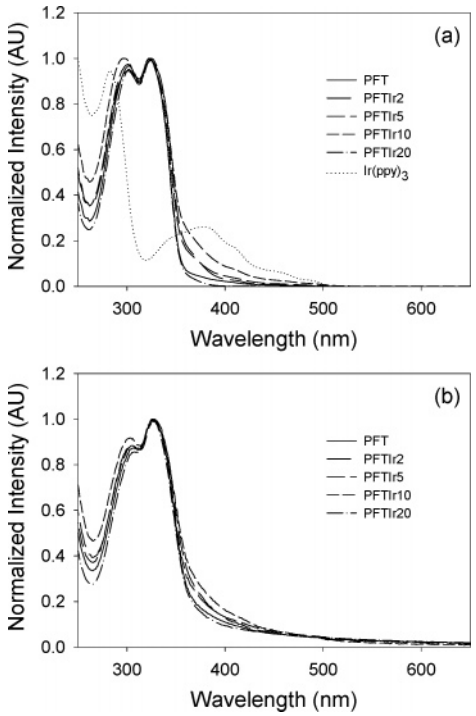

Figure 3. Absorption spectra of PFTIr in solution (a) and as a film (b).

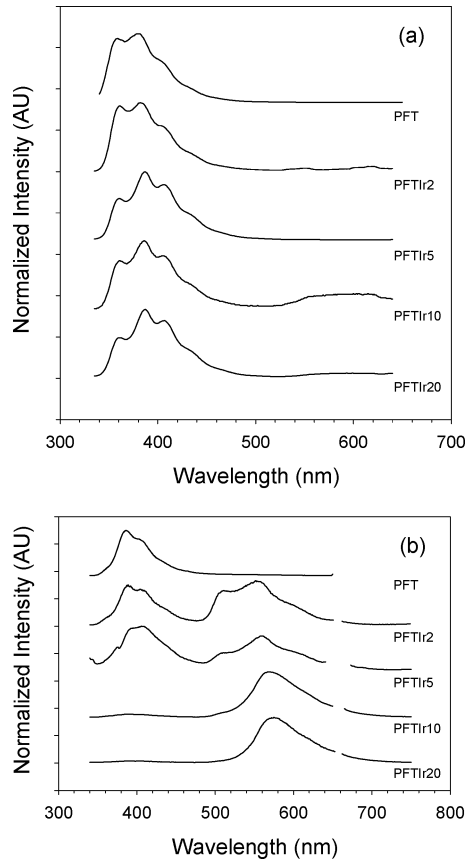

Figure 4. Photoluminescence spectra of PFTIr in solution (a) and as a film (b).

Absorption and Photoluminescent Properties. Incorporation of a less conjugated thienyl moiety into the polymer

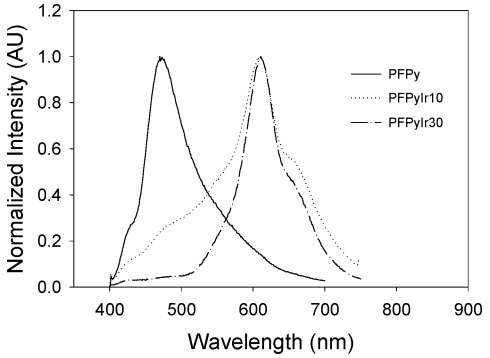

Figure 5. EL spectra of PFPyIr-based devices.

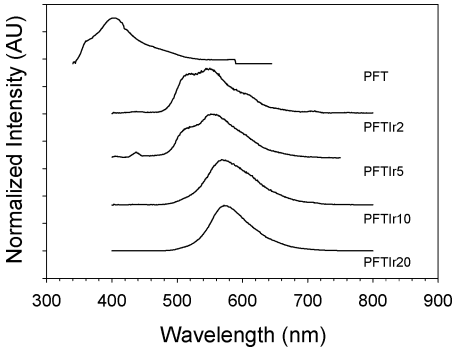

Figure 6. EL spectra of PFTIr-based devices.

backbone led to a significant change in spectroscopic properties relative to poly(9,9-dihexylfluorene-*alt*-pyridine) (PFPy). These spectroscopic changes are not believed to be due to the lower molecular weight of the PFTs compared to the PFPys (5000 vs 40000 Da). Work by Miller and Klaerner[29] supports this claim in their study of the effect of molecular weight on absorption and emission of oligo and poly(fluorene)s. As *n*, the number of repeat units, increases from 5 to 10, a small red shift is observed in the absorption maxima, and there is no change in the emission maxima. When $n > 10$, there is essentially no change in the absorption or emission maxima. The UV/vis absorption of PFT was blue-shifted relative to PFPy by 68 nm in both the solution and solid state (323 vs 391 nm and 326 vs 394 nm for PFT and PFPy). For the PFTIr series of materials, UV/vis absorption is dominated by the host polymer (PFT) since both materials absorb at 323 nm, while a small red shift is observed for films of the polymer (323 nm vs 326 nm). The photoluminescent properties were also affected by the presence of the thienyl group. The emission maxima were blue-shifted relative to PFPy by 36 and 38 nm in solution and solid state, respectively (380 vs 416 nm and 390 vs 428 nm for PFT and PFPy). Incorporation of iridium complexes into the polymer chain resulted in very little change in the solution or solid state absorption spectra (323 and 328 nm, respectively); however, significant changes are observed in the emission spectra (Figure 4). In solution, a broad weak emission peak can be seen at ~590 nm, while in the solid state, a strong emission is observed between 553 and 573 nm, depending on the content of iridium in the polymer. It should be noted that the fluorescence peak seen at 390 nm did not show any red shift as the iridium content increased, whereas the phosphorescence peak red-shifted by up to 20 nm. The latter is believed to be caused by an increase in conjugation length that does not appear to affect the fluorescence emission wavelength. It is concluded that the less conjugated thienyl segments isolate the emission from the fluorene backbone moiety. The increase in quantum yields of the PFTIr series relative to the PFPyIr series supports the hypothesis that emission quenching is reduced by changing the relative triplet energies of the host polymer and the phosphorescent guest.

Triplet Energies. The HOMO and LUMO energy levels of PFT (Scheme 5) were estimated as previously described. The ground state energy level of the iridium complex attached to PFT is approximated by that of $Ir(ppy)_3$ (5.2 eV)[30] due to the similarity of their chemical structures. The triplet energy of the phosphor was estimated from the phosphorescent emission wavelength (560 nm, 2.22 eV).

As illustrated by Scheme 5, the triplet energy of PFPy is lower than that of PFT. It should be noted that the triplet energies of the polymers are only approximations; it is the relative difference between triplet energies that are important and not their absolute values. The triplet state energy of PFT, incorporating the 3,4-linked thienyl, is ~0.7 eV larger than the corresponding triplet energy of the phosphor. Thus, the possibility of triplet energy transfer from an excited-state phosphor to the nonemitting triplet state of the backbone is reduced. In support of this hypothesis, the quantum yields of phosphorescence from PFTIr materials are found to be ~3 times greater (0.20) than those of the corresponding PFPyIr polymers.

Electroluminescence. Electroluminescence (EL) of the host polymer, PFPy, exhibits an emission maximum at 490 nm, which is red-shifted by 62 nm compared to its PL maximum (428 nm), as shown in Figure 5 and reported in Table 3. This is in agreement with previous reports in the literature[32] and may be explained by exciplex formation at the interfacial region when the emission wavelength becomes voltage dependent (Figure 5).[33] Incorporation of the iridium complex into the PFPy backbone results in a red-shifted emission at 610 nm which originates from the metal complex. At lower iridium concentrations, a subpeak at 490 nm is observed, as shown in Figure 5. The EL of the host polymer for the PFTIr series, PFT, has an emission maximum at 402 nm (see Table 3 and Figure 6). Incorporation of iridium complex results in emission from the lowest energy state of the system, the iridium complex. The emission maximum increases from 550 to 570 nm as the iridium content increases. Polymer PFTIr5 also displays a weak emission between 400 and 450 nm due to incomplete energy transfer. The PL and EL maximum emission wavelengths for all the polymers (Table 3) are quite similar to the exception of PFPy. However, the relative intensities of polymer host and the iridium complex are different.

EL can be generated by charge trapping or energy transfer,[34] which may result in significant differences in PL and EL emission for a given material. When the PL and EL spectra are similar, it can be concluded that the dominate mechanism generating luminescence is energy transfer, i.e., from the excited state of the polymer backbone to the emitting species. If the PL and EL spectra are different, as observed in the present system, then the dominate mechanism leading to luminescence is charge trapping. This may occur in a system with two different segments of differing energy levels; electrons or holes may be trapped on the lower energy segment. This causes a buildup of local charge density, which can in turn enhance the possibility of attracting the opposite charge carriers.[35] In addition to direct charge trapping, excitons formed on higher energy segments can undergo energy transfer to the lower energy sites. Direct and indirect charge trapping results in an increase in emission intensities from the emitting guest, relative to the polymer backbone, as observed in Figures 5 and 6.

Device Performance. Devices were fabricated using the following two configurations: ITO/PEDOT:PSS/polymer/CsF/Al and ITO/PEDOT:PSS/Polymer/TPBI/CsF/Al, where TPBI

Table 3. Summary of ITO/PEDOT:PSS/Polymer/CsF/Al Device Performance

	λ_{max} PL	λ_{max} EL	turn-on voltage (V)	max brightness (cd/m^2)	luminescence efficiency (cd/A)	external quantum efficiency (%)
PFPy	428 (453)	490	4.6	77	0.08	0.05
PFPyIr5	613 (423, 665)	609 (427)				
PFPyIr10	613 (423, 665, 453)	610 (458)				
PFPyIr20	613 (423, 665, 453)		3.8	48	0.02	
PFPyIr30	613 (423, 665, 453)	610	6.6	150	0.48	0.32
PFT	390, 410	402	27	1.80	0.003	
PFTIr2	553 (390, 410)	550	4.8	1274	0.80	0.24
PFTIr5	554 (410)	550	6.1	230	0.33	0.10
PFTIr10	570	568	7.0	1289	2.69	0.84
PFTIr20	573	572	6.7	1552	1.35	0.41

Table 4. Summary of ITO/PEDOT:PSS/Polymer/TPBI/CsF/Al Device Performance

	turn-on voltage (V)	max brightness (cd/m^2)	luminescence efficiency (cd/A)	external quantum efficiency (%)
PFT	21.5	9.39	0.02	
PFTIr2	8.3	3132	1.52	0.45
PFTIr5	6.4	291	0.66	0.21
PFTIr10	6.3	4541	4.11	1.29
PFTIr20	4.2	3462	1.94	0.59

represents (1,3,5-tris(*N*-phenylbenzimidazol-2-yl)benzene). Polymers from the PFPy series containing iridium, PFPyIr20 and PFPyIr30, show better device performance than the host polymer (PFPy). PFPyIr30 is twice as bright as the host at about 1/10 the current density. However, the maximum brightness obtained for the PFPyIr series is only ~100 cd/m^2, and furthermore the efficiencies are low (~0.5 cd/A) (see Table 3). These values are nevertheless comparable to similar systems that have been recently published.[17]

The PFTIr series also show much better device performances than their corresponding host polymers, i.e., in the absence of the Ir complex. The increase in performance is more drastic than the PFPyIr case because of the presence of the nonconjugated thiophene moiety in PFT. The host polymer, PFT, is a blue emitter but turn-on voltages are high (as high as 27 V) and the maximum brightness was only 9.4 cd/m^2. However, when the Ir complex is incorporated into the polymer, a considerable improvement in device performance is observed: the turn-on voltage is reduced by greater than one-half, and the brightness increased by 3 orders of magnitude (see Table 3). When comparing the relative current densities and brightnesses of PFTIr polymers, it can be concluded that PFTIr10 displays the best device performance and PFTIr5 the worst. At low current densities (0.04 A/cm^2), high brightnesses are obtained (1289 and 4541 cd/m^2) for PFTIr10 for device structures with and without a TPBI layer, and the efficiencies are 2.69 and 4.11 cd/A, respectively (see Tables 3 and 4).

For such a basic PLED structure, the performance of the PFTIr series is quite good and is attributed to the higher energy triplet energy of the polymer backbone. From a materials perspective, it is reasonable to conclude that further improvements may be achieved by using a phosphorescent emitter that has a low triplet energy state. On the other hand, device performances may also be improved by modifying the device structure. In this case, TPBI was introduced as a hole blocking layer with the intent to balance hole and electron flow. Typically, introduction of TPBI leads to a decrease in current densities,[36] but in this case a significant increase was observed. It is possible that this is due to the TPBI layer acting as an electron injector as well as a hole blocker. Both brightness and efficiency were increased by a factor of ~2. The device data reported in this paper are preliminary and provide an indication of the materials properties; refinement of the device configuration can be used to further optimize the PLED device performance.

Conclusion

Two different synthetic methods have been successfully used to yield two different iridium-containing conjugated polymers. One is a red-emitting conjugated polymer and the other a greenish-yellow emitter. A mechanism of energy transfer from the polymer backbone to the iridium complex, intersystem crossing, and phosphorescence from the Ir complex is assumed to be operating. Photoluminescence data indicate that emission quenching from the polymer triplet state occurs. It was found that increasing the triplet energy of the conjugated backbone by incorporation of a 3,4-linked thienyl group raises the energy of the triplet state of the polymer, thereby decreasing triplet energy transfer from the phosphorescent emitter to the nonemitting polymer backbone. Electroluminescence data indicate that charge trapping is the dominate mechanism occurring in the PLEDs, resulting in tunable emission color depending on the polymer structure.

Acknowledgment. We thank SFU and NSERC for financial assistance. A special thanks to Chih-Wei (Tony) Huang for his help and advice in LED fabrication and testing.

References and Notes

(1) Heeger, A. J. *Solid State Commun.* **1998**, *107*, 673.
(2) Ho, P. K. H.; Thomas, D. S.; Friend, R. H.; Tessler, N. *Science* **1999**, *285*, 233.
(3) Lamansky, S.; Djurovich, P. I.; Murphy, D.; Abdel-Razzaq, F.; Lee, H.-E.; Adachi, C.; Burrows, P. E.; Forrest, S. R.; Thompson, M. E. *J. Am. Chem. Soc.* **2001**, *123*, 4304.
(4) Niu, Y.-H.; Tung, Y.-L.; Chi, Y.; Shu, C.-f.; Kim, J. H.; Chen, B.; Luo, J.; Carty, A. J.; Jen, A. K.-Y. *Chem. Mater.* **2005**, *17*, 3532.
(5) Yang, J.; Gordon, K. C. *Synth. Met.* **2005**, *152*, 213.
(6) Li, F.; Zhang, M.; Cheng, G.; Zhao, Y.; Feng, J.; Ma, Y. G.; Liu, S. Y.; Shen, J. C. *Appl. Phys. Lett.* **2004**, *84*, 147.
(7) Brooks, J.; Babayan, Y.; Lamansky, S.; Djurovich, P. I.; Tsyba, I.; Bau, R.; Thompson, M. E. *Inorg. Chem.* **2002**, *41*, 3055.
(8) Lee, C. L.; Lee, K. B.; Kim, J. J. *Appl. Phys. Lett.* **2000**, *77*, 2280.
(9) Gong, X.; Ostrowski, J. C.; Bazan, G. C.; Moses, D.; Heeger, A. J.; Lui, M. S.; Jen, A. K.-Y. *Adv. Mater.* **2003**, *15*, 45−49 and references therein.
(10) Chen, F. C.; He, G.; Yang, Y. *Appl. Phys. Lett.* **2003**, *82*, 1006.
(11) Sandee, A. J.; Willianms, C. K.; Evans, N. R.; Davies, J. E.; Boothby, C. E.; Köhler, A.; Friend, R. H.; Holmes, A. B. *J. Am. Chem. Soc.* **2004**, *126*, 7041.
(12) Zhen, H.; Jiang, C.; Yang, W.; Jiang, J.; Huang, F.; Cao, Y. *Chem.—Eur. J.* **2005**, *11*, 5007.
(13) Chen, X.; Liao, J.-L.; Liang, Y.; Ahmed, M. O.; Tseng, H.-E.; Chen, S.-A. *J. Am. Chem. Soc.* **2003**, *125*, 636.
(14) Jiang, J.; Jiang, C.; Yang, W.; Zhen, H.; Huang, F.; Cao, Y. *Macromolecules* **2005**, *38*, 4072.
(15) Sudhakar, M.; Djurovich, P. I.; Hogen-Esch, T. E.; Thompson, M. E. *J. Am. Chem. Soc.* **2003**, *125*, 7796.
(16) Yang, W.; Zhen, H. Y.; Jiang, C. Y.; Su, L. J.; Jiang, J. X.; Shi, H. H.; Cao, Y. *Synth. Met.* **2005**, *153*, 189.
(17) Ito, T.; Suzuki, S.; Kido, J. *Polym. Adv. Technol.* **2005**, *16*, 480.
(18) Ranger, M.; Leclerc, M. *Can. J. Chem.* **1998**, *76*, 1571.

(19) Vamvounis, G.; Schulz, G. L.; Holdcroft, S. *Macromolecules* **2004**, *37*, 8897.
(20) Tokito, S.; Suzuki, M.; Tanaka, I.; Inoue, Y.; Shirane, K.; Takeuchi, M.; Ito, N. US 2003/0091862A1, May 15, 2003.
(21) Saito, K.; Matsusue, N.; Kanno, H.; Hamada, Y.; Takahashi, H.; Matsumura, T. *Jpn. J. Appl. Phys.* **2004**, *43*, 2733.
(22) Yamamoto, T.; Zhou, Z.-H.; Kanbara, T.; Shimura, M.; Kizu, K.; Maruyama, T.; Nakamura, Y.; Fukuda, T.; Lee, B.-L.; Ooba, N.; Tomaru, S.; Kurihara, T.; Kaino, T.; Kubota, K.; Sasaki, S. *J. Am. Chem. Soc.* **1996**, *118*, 10389.
(23) Konno, H.; Sasaki, Y. *Chem. Lett.* **2003**, *32*, 252.
(24) Tamayo, A. B.; Alleyne, B. D.; Djurovich, P. I.; Lamansky, S.; Tsyba, I.;Ho, N. N.; Bau, R.; Thompson, M. E. *J. Am. Chem. Soc.* **2003**, *125*, 7377.
(25) Baldo, M. A.; Thompson, M. E.; Forrest, S. R. *Pure Appl. Chem.* **1999**, *17*, 2095.
(26) Neher, D. *Macromol. Rapid Commun.* **2001**, *22*, 1365.
(27) Lamansky, S.; Djurovich, P. I.; Murphy, D.; Abdel-Razzaq, F.; Kwong, R.; Tsyba, I.; Bortz, M.; Mui, B.; Bau, R.; Thompson, M. E. *Inorg. Chem.* **2001**, *40*, 1704.
(28) Lui, B.; Yu, W.-L.; Lai, Y.-H.; Huang, W. *Chem. Mater.* **2001**, *13*, 1984.
(29) Klaerner, G.; Miller, R. D. *Macromolecules* **1998**, *31*, 2007.
(30) Mäkinen, A. J.; Hill, I. J.; Kafafi, Z. H. *J. Appl. Phys.* **2002**, *92*, 1598.
(31) Monkman, A. P.; Burrows, H. D.; Hartwell, L. J.; Horsburgh, L. E.; Hamblett, I.; Navaratnam, S. *Phys. Rev. Lett.* **2001**, *86*, 1358.
(32) Aubert, P.-H.; Knipper, M.; Groenendaal, L.; Lutsen, L.; Manca, J.; Vanderzande, D. *Macromolecules* **2004**, *37*, 4087.
(33) Donat-Bouillud, A.; Levesque, I.; Tao, Y.; D'Iorio, M.; Beaupre, S.; Blondin, P.; Ranger, M.; Bouchard, J.; Leclerc, M. *Chem. Mater.* **2000**, *12*, 1931.
(34) Gong, X.; Lim, S.-H.; Ostrowski, J. C.; Moses, D.; Bardeen, C. J.; Bazan, G. C. *J. Appl. Phys.* **2004**, *95*, 3, 950.
(35) Liu, M. S.; Luo, J.; Jen, A. K.-Y. *Chem. Mater.* **2003**, *15*, 3496.
(36) Huang, T.-H.; Lin, J. T.; Tao, Y.-H.; Chuen, C.-H. *Chem. Mater.* **2003**, *15*, 4854.

MA061814O